Scientia Iranica, Vol. 14, No. 5, pp 385 394

SCIENTIA IRANICA

Dynamic Responses of Railway Suspension Bridges Under Moving Trains

H. Xia[1], Y.L. Xu[2], T.H.T. Chan[2] and J.A. Zakeri[*]

This paper describes a numerical simulation technique that is used to investigate a dynamic train-long suspension bridge interaction. A three-dimensional finite element model is used to represent a long suspension bridge. Each vehicle of the train is modeled by a 27-degrees-of-freedom dynamic system, including two bogies with four wheel-sets. By applying a mode superposition technique to the bridge and taking the measured wheel and track irregularities as known quantities, the degrees of freedom of the bridge-train system are significantly reduced and the coupled equations of motion are efficiently solved. The proposed formulation and the associated computer program are then applied to a real long suspension bridge. The dynamic responses of the bridge and the train vehicles are computed and compared with the limited measured data and the results are satisfactory.

INTRODUCTION

To meet the needs of modern society for advanced transportation systems, more and more long suspension bridges have been built throughout the world, such as the Minami Bisan Seto suspension bridge in Japan in 1988 [1] and the Tsing Ma suspension bridge in Hong Kong in 1997 [2]. For such long span bridge-train systems, Diana and Cheli [3] pointed out two fundamental aspects to be investigated: One is bridge safety, due to train passage and the other is train runability, including passenger comfort.

In this paper, a three-dimensional model is presented, first, for investigating the dynamic interaction of long suspension bridges with moving trains. The measured irregularities between wheels and track are used to represent their non-linear relationship and are taken as known quantities. The modal superposition technique is applied to the bridge, which further reduces computational effort. This formulation, together with the associated computer program is, then, applied to a real long suspension bridge carrying a railway within the bridge deck as a case study. Finally, the computed bridge response is compared with the limited measured results to verify the approach, to some extent.

1. *School of Civil Engineering & Architecture, Beijing Jiaotong University, Beijing, China.*
2. *Department of Civil and Structural Engineering, Hong Kong Polytechnic University, Hong Kong, China.*
*. *Corresponding Author, School of Railway Engineering, Iran University of Science & Technology, Tehran, I.R. Iran.*

BASIC DYNAMIC MODELS

Dynamic Model of Train

The dynamic model of a train consists of several locomotives, passenger coaches or freight cars. Each vehicle is composed of a car body, bogies, wheel-sets and the connections between the components [4]. The following assumptions are used in the modeling of the train in this study (see Figure 1):

1. The car body, bogies and wheel-sets in each vehicle are regarded as rigid components;
2. The connections of car body-bogies and the connections of bogie-wheel-sets are represented by linear springs and viscous dashpots.

With the above assumptions, the ith vehicle body has five degrees of freedom with which to be concerned. They are designated by the lateral displacement, Y_{ci}, roll displacement, θ_{ci}, yaw displacement, Ψ_{ci}, vertical displacement, Z_{ci}, and pitch displacement, φ_{ci}. The jth bogie in the ith vehicle has five degrees of freedom:

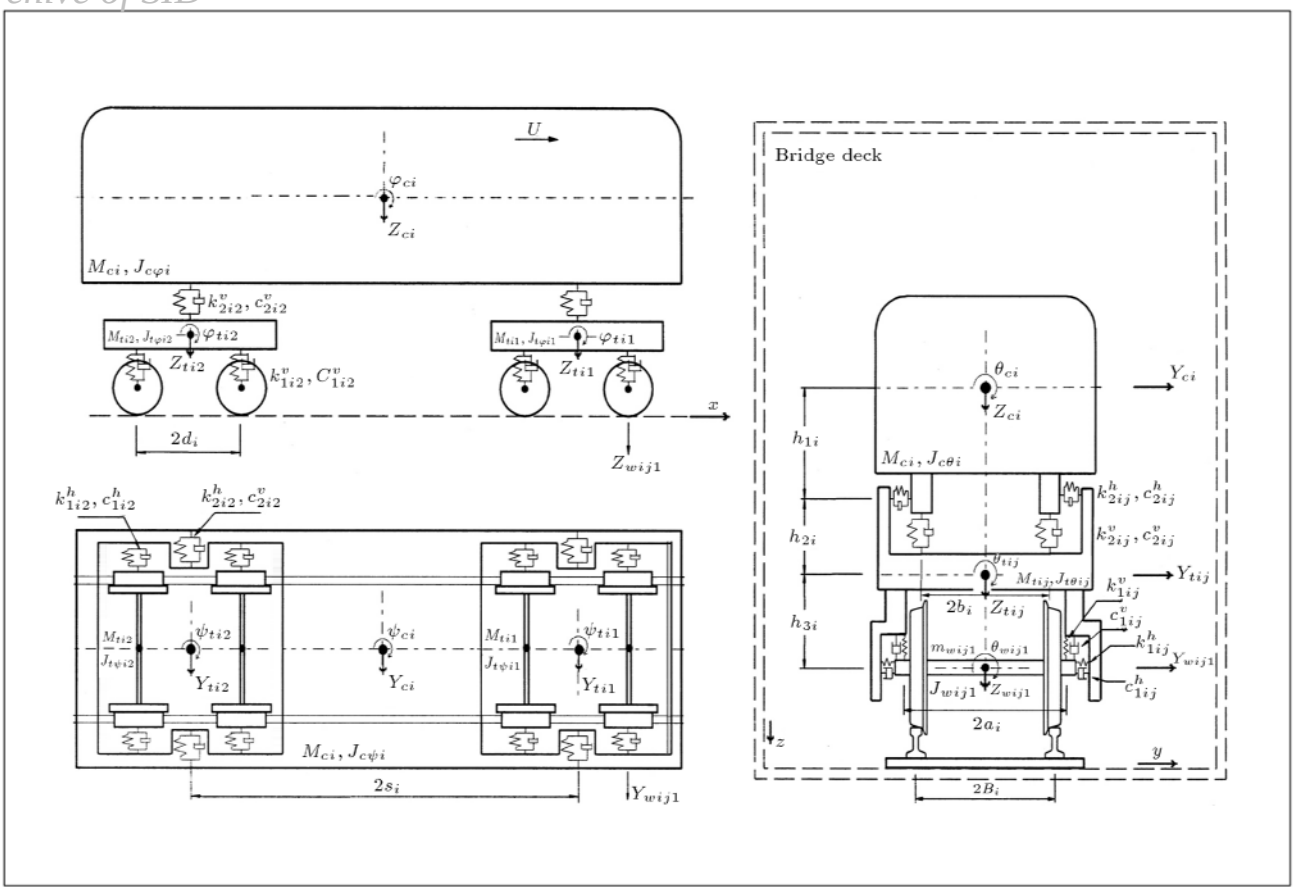

Figure 1. Dynamic model of vehicle.

The lateral displacement, Y_{tij}, roll displacement, θ_{tij}, yaw displacement, Ψ_{tij}, vertical displacement, Z_{tij}, and pitch displacement, φ_{tij}. For the lth wheel in the jth bogie and ith vehicle, only three degrees of freedom are considered: The lateral displacement, Y_{wij1}, roll displacement, θ_{wij1}, and vertical displacement, Z_{wij1}.

For a 4-axle 2-bogies vehicle studied in this paper, the total degrees of freedom are twenty-seven [5]. The equations of motion for the car body and two bogies in the ith vehicle can be derived, as follows:

$$\begin{bmatrix} \mathbf{M}_{cci} & 0 & 0 \\ 0 & \mathbf{M}_{t_1t_1i} & 0 \\ 0 & 0 & \mathbf{M}_{t_2t_2i} \end{bmatrix} \begin{Bmatrix} \ddot{\mathbf{v}}_{ci} \\ \ddot{\mathbf{v}}_{t_1i} \\ \ddot{\mathbf{v}}_{t_2i} \end{Bmatrix} + \begin{bmatrix} \mathbf{C}_{cci} & \mathbf{C}_{t_1ci} & \mathbf{C}_{t_2ci} \\ \mathbf{C}_{ct_1i} & \mathbf{C}_{t_1t_1i} & 0 \\ \mathbf{C}_{ct_2i} & 0 & \mathbf{C}_{t_2t_2i} \end{bmatrix} \begin{Bmatrix} \dot{\mathbf{v}}_{ci} \\ \dot{\mathbf{v}}_{t_1i} \\ \dot{\mathbf{v}}_{t_2i} \end{Bmatrix} + \begin{bmatrix} \mathbf{K}_{cci} & \mathbf{K}_{t_1ci} & \mathbf{K}_{t_2ci} \\ \mathbf{K}_{ct_1i} & \mathbf{K}_{t_1t_1i} & 0 \\ \mathbf{K}_{ct_2i} & 0 & \mathbf{K}_{t_2t_2i} \end{bmatrix} \begin{Bmatrix} \mathbf{v}_{ci} \\ \mathbf{v}_{t_1i} \\ \mathbf{v}_{t_2i} \end{Bmatrix} = \begin{Bmatrix} \mathbf{F}_{ci} \\ \mathbf{F}_{t_1i} \\ \mathbf{F}_{t_2i} \end{Bmatrix}, \quad (1)$$

where the subscripts c, t_1 and t_2 represent the car body and the front and rear bogies of the vehicle, respectively, $i = 1, 2, \cdots N_v$, and N_v is the number of vehicles on the bridge.

The sub-mass diagonal matrices and the sub-stiffness matrices are expressed, as follows:

$$M_{cci} = \text{diag}\left[M_{ci} \quad J_{c\theta i} \quad J_{c\psi i} \quad M_{ci} \quad J_{c\varphi i}\right],$$

and:

$$M_{t_jt_ji} = \text{diag}\left[M_{tij} \quad J_{t\theta ij} \quad J_{t\psi ij} \quad M_{tij} \quad J_{t\varphi ij}\right], \quad (2)$$

$$\mathbf{K}_{cci} = \begin{bmatrix} k^h_{2i1}+k^h_{2i2} & (k^h_{2i1}+k^h_{2i2}) & 0 & 0 & 0 \\ (k^h_{2i1}+k^h_{2i2}) & h^2_{1i}(k^h_{2i1}+k^h_{2i2})+b^2_i(k^v_{2i1}+k^v_{2i2}) & 0 & 0 & 0 \\ 0 & 0 & s^2_i(k^h_{2i1}+k^h_{2i2}) & 0 & 0 \\ 0 & 0 & 0 & k^v_{2i1}+k^v_{2i2} & 0 \\ 0 & 0 & 0 & 0 & s^2_i(k^v_{2i1}+k^v_{2i2}) \end{bmatrix}, \quad (3)$$

$$\mathbf{K}_{t_j t_j i} =$$

$$\begin{bmatrix} k_{2ij}^h + 2k_{1ij}^h & h_{2i}k_{2ij}^h & 2h_{3i}k_{1ij}^h \\ h_{2i}k_{2ij}^h & 2h_{3i}k_{1ij}^h & h_{2i}^2 k_{2ij}^h + b_i^2 k_{2ij}^v + 2h_{3i}^2 k_{1ij}^h + 2a_i^2 k_{1ij}^v \\ 0 & 0 & \\ 0 & 0 & \\ 0 & 0 & \end{bmatrix}$$

$$\begin{bmatrix} 0 & 0 & 0 \\ 0 & 0 & 0 \\ 2d_i^2 k_{1ij}^h & 0 & 0 \\ 0 & 2k_{1ij}^v + k_{2ij}^v & 0 \\ 0 & 0 & 2d_i^2 k_{1ij}^v \end{bmatrix}, \tag{4}$$

$$\mathbf{K}_{ct_1} = \mathbf{K}_{t_1 c}^T =$$

$$\begin{bmatrix} k_{2i1}^h & h_{1i}k_{2i1}^h & s_i k_{2i1}^h \\ h_{2i}k_{2i1}^h & h_{1i}h_{2i}k_{2i1}^h & b_i^2 k_{2i1}^v & h_{2i}s_i k_{2i1}^h \\ 0 & 0 & 0 \\ 0 & 0 & 0 \\ 0 & 0 & 0 \end{bmatrix}$$

$$\begin{bmatrix} 0 & 0 \\ 0 & 0 \\ 0 & 0 \\ k_{2i1}^v & s_i k_{2i1}^v \\ 0 & 0 \end{bmatrix}, \tag{5}$$

$$\mathbf{K}_{ct_2} = \mathbf{K}_{t_2 c}^T =$$

$$\begin{bmatrix} k_{2i2}^h & h_{1i}k_{2i2}^h & s_i k_{2i2}^h \\ h_{2i}k_{2i2}^h & h_{1i}h_{2i}k_{2i2}^h & b_i^2 k_{2i2}^v & h_{2i}s_i k_{2i2}^h \\ 0 & 0 & 0 \\ 0 & 0 & 0 \\ 0 & 0 & 0 \end{bmatrix}$$

$$\begin{bmatrix} 0 & 0 \\ 0 & 0 \\ 0 & 0 \\ k_{2i2}^v & s_i k_{2i2}^v \\ 0 & 0 \end{bmatrix}. \tag{6}$$

The sub-damping matrix can be obtained by simply replacing "k" in the corresponding sub-stiffness matrix by "c". $\mathbf{v}_i$, $\dot{\mathbf{v}}_i$ and $\ddot{\mathbf{v}}_i$ are the displacement, velocity and acceleration vectors of the ith vehicle, respectively.

The force vector consists of two parts:

$$\begin{Bmatrix} \mathbf{F}_{ci} \\ \mathbf{F}_{t_1 i} \\ \mathbf{F}_{t_2 i} \end{Bmatrix} = \begin{Bmatrix} \mathbf{F}_{cei} \\ \mathbf{F}_{t_1 ei} \\ \mathbf{F}_{t_2 ei} \end{Bmatrix} + \begin{Bmatrix} \mathbf{0} \\ \mathbf{F}_{t_1 wi} \\ \mathbf{F}_{t_2 wi} \end{Bmatrix}. \tag{7}$$

The components in the first part, $\mathbf{F}_{cei}$, $\mathbf{F}_{t_1 ei}$ and $\mathbf{F}_{t_2 ei}$, are the vectors of external forces (such as wind forces) acting on the car body and the front and rear bogies of the vehicle, respectively. $\mathbf{F}_{t_1 wi}$ and $F_{t_2 wi}$ are the vectors of forces transmitted from the wheels through the primary springs and dashpots to the front and rear bogies, respectively. The forces transmitted from all of their wheels to the bogies can be expressed in terms of the displacements and velocities of the wheels.

$$\mathbf{F}_{t_j wi} = \sum_{l=1}^{N_{wij}}$$

$$\begin{Bmatrix} (k_{1ij}^h Y_{wijl} + c_{1ij}^h \dot{Y}_{wijl}) \\ 2a_i^2 (k_{1ij}^v \theta_{wijl} + c_{1ij}^v \dot{\theta}_{wijl}) \quad h_{4i}(k_{1ij}^h Y_{wijl} + c_{1ij}^h \dot{Y}_{wijl}) \\ 2\eta_l d_i (k_{1ij}^h Y_{wijl} + c_{1ij}^h \dot{Y}_{wijl}) \\ (k_{1ij}^v Z_{wijl} + c_{1ij}^v \dot{Z}_{wijl}) \\ 2\eta_l d_i (k_{1ij}^v Z_{wijl} + c_{1ij}^v \dot{Z}_{wijl}) \end{Bmatrix},$$

$$j = 1, 2, \tag{8}$$

where N_{wij} is the number of wheel-sets in the jth bogie of the ith vehicle. η_l is the sign function, with $\eta_l = 1$ when the wheel is in the front bogie and $\eta_l = \quad 1$ when it is in the rear bogie.

Dynamic Model of Suspension Bridge

A long suspension bridge consists of bridge towers, bridge deck, cables, suspenders and anchorages. This study assumes that there is no relative displacement between the track and bridge deck. Using the finite element method, the equation of motion for the bridge can be expressed, as follows:

$$\mathbf{M}\ddot{\mathbf{X}} + \mathbf{C}\dot{\mathbf{X}} + \mathbf{K}\mathbf{X} = \mathbf{F}, \tag{9}$$

where $\mathbf{F}$ is the force vector, consisting of two parts, $\mathbf{F} = \mathbf{F}_e + \mathbf{F}_w$. $\mathbf{F}_e$ is the vector of external forces acting on the nodes of the bridge model and $\mathbf{F}_w$ is the vector of forces from the wheels of a train on the bridge deck through the track. The displacements of the bridge deck at any section in the finite element analysis are usually identified in terms of the lateral displacement, Y_b, vertical displacement, Z_b, and torsional displacement, θ_b, at the shear center (or centroid) of the cross section [6]. The lateral, vertical and torsional forces given by the lth wheel in the jth bogie of the ith vehicle, corresponding to the deck displacements, can be expressed, as follows:

$$\begin{aligned} F_{hijl} = \quad & m_{wijl}\ddot{Y}_{wijl} + c_{1ij}^h(\dot{Y}_{t_j i} \quad 00h_{3i}\dot{\theta}_{t_j i} \\ & + 2\eta_l d_i \dot{\psi}_{t_j i} \quad \dot{Y}_{wijl}) \\ & + k_{1ij}^h(Y_{t_j i} \quad h_{3i}\theta_{t_j i} + 2\eta_l d_i \psi_{t_j i} \quad Y_{wijl}), \end{aligned}$$

$$F_{vijl} = m_{wijl}\ddot{Z}_{wijl} + c^v_{1ij}(\dot{Z}_{t_ji} + 2\eta_l d_i\dot{\varphi}_{t_ji} - \dot{Z}_{wijl}) + k^v_{1ij}(Z_{t_ji} + 2\eta_l d_i\varphi_{t_ji} - Z_{wijl}) + g[m_{wijl} + (0.5M_{ci} + M_{t_ji})/N_{wij}],$$

$$F_{\theta ijl} = F'_{\theta ijl} + h_{4i}F_{hijl} + e_iF_{vijl} = J_{wijl}\ddot{\theta}_{wijl} + 2a_i^2c^v_{1ij}(\dot{\theta}_{t_ji} - \dot{\theta}_{wijl}) + 2a_i^2k^v_{1ij}(\theta_{t_ji} - \theta_{wijl}) + h_{4i}F_{hijl} + e_iF_{vijl}, \quad (10)$$

where g is the acceleration, due to gravity.

Wheel Hunting and Track Irregularities

Track irregularity is an important source of self-excitation in the bridge-train system. The track irregularities consist of lateral irregularity, $Y_s(x)$, vertical irregularity, $Z_s(x)$, and rotational irregularity, $\theta_s(x)$. In this study, the measured track irregularities are used so that these functions are regarded as known quantities. In consideration of track irregularities, the relations between the lth wheel displacements and the bridge deck displacements can be deduced, as follows:

$$\begin{Bmatrix} Y_{wijl} \\ \theta_{wijl} \\ Z_{wijl} \end{Bmatrix} = \begin{Bmatrix} Y_b(x_{ijl}) + h_{4i}\theta_b(x_{ijl}) + Y_s(x_{ijl}) \\ \theta_b(x_{ijl}) + \theta_s(x_{ijl}) \\ Z_b(x_{ijl}) + e_i\theta_b(x_{ijl}) + Z_s(x_{ijl}) \end{Bmatrix}, \quad (11)$$

where, x_{ijl} is the coordinate of the lth wheel of the jth bogie in the ith vehicle along the bridge deck.

EQUATIONS OF MOTION FOR BRIDGE-TRAIN SYSTEM

This study concerns the dynamic interaction between the suspension bridge and train and no external excitations, such as wind or earthquake, are included. Equations 1 to 11 constitute the basic equations for the coupled bridge-train system. However, the direct integration of these equations in the time domain, to find the dynamic responses of both the bridge and the train, is very cumbersome. The mode superposition method is, therefore, used in this study for the bridge [7,8]. The mode shape between the deck nodes can be determined using the Lagrange interpolation.

Let $\phi^n_h(x_{ijl})$, $\phi^n_\theta(x_{ijl})$ and $\phi^n_v(x_{ijl})$ denote the values of the lateral, rotational and vertical components of the nth bridge mode at the position of the lth wheel of the jth bogie in the ith vehicle, and q_n the generalized coordinate of the nth mode. The displacement of the bridge deck at the same position can be expressed, as follows:

$$Y_b(x_{ijl}) = \sum_{n=1}^{N_b} q_n\phi^n_h(x_{ijl}),$$

$$\theta_b(x_{ijl}) = \sum_{n=1}^{N_b} q_n\phi^n_\theta(x_{ijl}),$$

$$Z_b(x_{ijl}) = \sum_{n=1}^{N_b} q_n\phi^n_v(x_{ijl}), \quad (12)$$

where N_b is the number of the mode shapes concerned. If the bridge mode shapes are normalized, as $\{\phi^n\}^T\mathbf{M}\{\phi^n\} = 1$, the equation of motion of the bridge deck related to the nth mode, Equation 9, can be derived, as follows:

$$\ddot{q}_n + 2\xi_n\omega_n\dot{q}_n + \omega_n^2q_n = F_n, \quad (13)$$

where ξ_n and ω_n are, respectively, the damping ratio and the circular frequency of the nth mode of the bridge and F_n is the nth generalized force.

$$F_n = \sum_{i=1}^{N_v}\sum_{j=1}^{2}\sum_{l=1}^{N_{wij}} F_{nijl} = \sum_{i=1}^{N_v}\sum_{j=1}^{2}\sum_{l=1}^{N_{wij}} \phi^n_h(x_{ijl})F_{hijl} + \phi^n_\theta(x_{ijl})F_{\theta ijl} + \phi^n_v(x_{ijl})F_{vijl}, \quad (14)$$

where F_{nijl} is the nth generalized force from the lth wheel of the jth bogie of the ith vehicle. Furthermore, in terms of Equation 12, the displacements of the lth wheel (Equation 11) can be expressed as the function of the generalized coordinate and mode shape of the bridge, as well as the known track irregularities.

$$\begin{Bmatrix} Y_{wijl} \\ \theta_{wijl} \\ Z_{wijl} \end{Bmatrix} = \sum_{n=1}^{N_b} \begin{Bmatrix} q_n[\phi^n_h(x_{ijl}) + h_{4i}\phi^n_\theta(x_{ijl})] \\ q_n\phi^n_\theta(x_{ijl}) \\ q_n[\phi^n_v(x_{ijl}) + e_i\phi^n_\theta(x_{ijl})] \end{Bmatrix} + \begin{Bmatrix} Y_s(x_{ijl}) + Y_h(x_{ijl}) \\ \theta_s(x_{ijl}) \\ Z_s(x_{ijl}) \end{Bmatrix}. \quad (15)$$

Clearly, the displacements of the wheel need not be included in the equations of motion for the bridge-train system. This can reduce the computational effort significantly. Combining the above equations and then carrying out some manipulation, one can derive the coupled equations of motion for the bridge-train system as:

$$\begin{bmatrix} \mathbf{M}_{vv} & 0 \\ 0 & \mathbf{M}_{bb} \end{bmatrix} \begin{Bmatrix} \ddot{\mathbf{X}}_v \\ \ddot{\mathbf{X}}_b \end{Bmatrix} + \begin{bmatrix} \mathbf{C}_{vv} & \mathbf{C}_{vb} \\ \mathbf{C}_{bv} & \mathbf{C}_{bb} \end{bmatrix} \begin{Bmatrix} \dot{\mathbf{X}}_v \\ \dot{\mathbf{X}}_b \end{Bmatrix} + \begin{bmatrix} \mathbf{K}_{vv} & \mathbf{K}_{vb} \\ \mathbf{K}_{bv} & \mathbf{K}_{bb} \end{bmatrix} \begin{Bmatrix} \mathbf{X}_v \\ \mathbf{X}_b \end{Bmatrix} = \begin{Bmatrix} \mathbf{F}_v \\ \mathbf{F}_b \end{Bmatrix}, \quad (16)$$

where the subscripts "v" and "b" represent the vehicles and bridge, respectively. Assuming that the number of vehicles on the bridge is N_v and the number of concerned bridge vibration modes is N_b, the sub-displacement vectors can be expressed as:

$$\mathbf{X}_v = \begin{bmatrix}\mathbf{X}_{v1} & \mathbf{X}_{v2} & \cdots & \mathbf{X}_{vN_v}\end{bmatrix}^T,$$

$$\mathbf{X}_b = \begin{bmatrix}q_1 & q_2 & \cdots & q_{N_b}\end{bmatrix}^T, \tag{17}$$

where $\mathbf{X}_{vi} = [\mathbf{v}_{ci},\ \mathbf{v}_{t_1 i},\ \mathbf{v}_{t_2 i}]^T,\ i = 1, 2, \ldots N_v$. The sub-mass and stiffness matrices of the vehicles are listed, as follows:

$$\mathbf{M}_{vv} = \begin{bmatrix}\mathbf{M}_{v1} & 0 & 0 & 0\\ 0 & \mathbf{M}_{v2} & 0 & 0\\ 0 & 0 & \ddots & 0\\ 0 & 0 & 0 & \mathbf{M}_{vN_v}\end{bmatrix},$$

$$\mathbf{K}_{vv} = \begin{bmatrix}\mathbf{K}_{v1} & 0 & 0 & 0\\ 0 & \mathbf{K}_{v2} & 0 & 0\\ 0 & 0 & \ddots & 0\\ 0 & 0 & 0 & \mathbf{K}_{vN_v}\end{bmatrix}, \tag{18}$$

where:

$$\mathbf{M}_{vi} = \begin{bmatrix}\mathbf{M}_{cci} & 0 & 0\\ 0 & \mathbf{M}_{t_1 t_1 i} & 0\\ 0 & 0 & \mathbf{M}_{t_2 t_2 i}\end{bmatrix},$$

$$\mathbf{K}_{vi} = \begin{bmatrix}\mathbf{K}_{cci} & \mathbf{K}_{t_1 ci} & \mathbf{K}_{t_2 ci}\\ \mathbf{K}_{ct_1 i} & \mathbf{K}_{t_1 t_1 i} & 0\\ \mathbf{K}_{ct_2 i} & 0 & \mathbf{K}_{t_2 t_2 i}\end{bmatrix}. \tag{19}$$

The sub-damping matrix of the vehicle can be achieved by simply replacing "$\mathbf{K}$" in the stiffness matrix by "$\mathbf{C}$".

The sub-mass, sub-stiffness and sub-damping matrices of the bridge are deduced, as follows:

$$\mathbf{M}_{bb} = \begin{bmatrix}1 + M_b^{11} & M_b^{12} & \cdots & M_b^{1N_b}\\ M_b^{21} & 1 + M_b^{22} & \cdots & M_b^{2N_b}\\ \cdots & \cdots & \ddots & \cdots\\ M_b^{N_b 1} & M_b^{N_b 2} & \cdots & 1 + M_b^{N_b N_b}\end{bmatrix},$$

$$\mathbf{K}_{bb} = \begin{bmatrix}\omega_1^2 + K_b^{11} & K_b^{12} & \cdots & K_b^{1N_b}\\ K_b^{21} & \omega_2^2 + K_b^{22} & \cdots & K_b^{2N_b}\\ \cdots & \cdots & \ddots & \cdots\\ K_b^{N_b 1} & K_b^{N_b 2} & \cdots & \omega_b^{N_b} + K_b^{N_b N_b}\end{bmatrix},$$

$$\mathbf{M}_b^{nm} = \sum_{i=1}^{N_v}\sum_{j=1}^{2}\sum_{l=1}^{N_{wij}} (\Phi_{hijl}^{nm} m_{wijl} + \phi_{\theta ijl}^{nm} J_{wijl} + \Phi_{vijl}^{nm} m_{wijl}),$$

$$K_b^{nm} = \sum_{i=1}^{N_v}\sum_{j=1}^{2}\sum_{l=1}^{N_{wij}} (\Phi_{hijl}^{nm} k_{1ij}^h + 2\phi_{\theta ijl}^{nm} k_{1ij}^v a_i^2 + \Phi_{vijl}^{nm} k_{1ij}^v),$$

$$\mathbf{C}_{bb} = \begin{bmatrix}2\xi\omega_1 + C_b^{11} & C_b^{12} & \cdots & C_b^{1N_b}\\ C_b^{21} & 2\xi\omega_2 + C_b^{22} & \cdots & C_b^{2N_b}\\ \cdots & \cdots & \ddots & \cdots\\ C_b^{N_b 1} & C_b^{N_b 2} & \cdots & 2\xi\omega_{N_b} + C_b^{N_b N_b}\end{bmatrix},$$

$$C_b^{nm} = \sum_{i=1}^{N_v}\sum_{j=1}^{2}\sum_{l=1}^{N_{wij}} (\Phi_{hijl}^{nm} c_{1ij}^h + 2\phi_{\theta ijl}^{nm} c_{1ij}^v a_i^2 + \Phi_{vijl}^{nm} c_{1ij}^v). \tag{20}$$

The sub-stiffness matrices attributed to the interaction between the bridge and the vehicles can be derived as:

$$\mathbf{K}_{vb} = \{\mathbf{K}_{bv}\}^T = \begin{bmatrix}\mathbf{K}_{vb1}\\ \mathbf{K}_{vb2}\\ \cdots\\ \mathbf{K}_{vbN_v}\end{bmatrix},$$

$$\mathbf{K}_{vbi} = \begin{bmatrix}0 & 0 & \cdots & 0\\ \mathbf{K}_{t_1 q1}^i & \mathbf{K}_{t_1 q2}^i & \mathbf{K}_{t_1 q N_b}^i\\ \mathbf{K}_{t_2 q1}^i & \mathbf{K}_{t_2 q2}^i & \mathbf{K}_{t_2 q N_b}^i\end{bmatrix},$$

$$\mathbf{K}_{t_j qn}^i = \{\mathbf{K}_{qnt_j}^i\}^T = \sum_{l=1}^{Nwij} \begin{bmatrix}(\phi_{hijl}^n + h_{4i}\phi_{\theta ijl}^n)k_{1ij}^h\\ 2\phi_{\theta ijl}^n a_i^2 k_{1ij}^v \quad h_{4i}\phi_{hijl}^n k_{1ij}^h\\ 2\eta_l d_i \phi_{hijl}^n k_{1ij}^h\\ (\phi_{vijl}^n + e_i\phi_{\theta ijl}^n)k_{1ij}^v\\ 2\eta_l d_i \phi_{vijl}^n k_{1ij}^v\end{bmatrix}, \tag{21}$$

where $i = 1, 2, \cdots N_v$, $n = 1, 2, \cdots N_b$ and $j = 1, 2$. The sub-damping matrices attributed to the interaction between the bridge and vehicles can be obtained by simply replacing "k" in Equation 21 by "c". If the external forces, such as wind and earthquake, are not taken into account, the force vectors can be expressed,

as follows:

$$\mathbf{F}_v = \begin{bmatrix}\mathbf{F}_{v1} & \mathbf{F}_{v2} & \cdots & \mathbf{F}_{vN_b}\end{bmatrix}^T,$$

$$\mathbf{F}_b = \begin{bmatrix}\mathbf{F}_{b1} & \mathbf{F}_{b2} & \cdots & \mathbf{F}_{bN_b}\end{bmatrix}^T,$$

$$\mathbf{F}_{vi} = \begin{bmatrix}0 & \mathbf{F}_{vi}^{t_1} & \mathbf{F}_{vi}^{t_2}\end{bmatrix}^T,$$

$$\mathbf{F}_{vi}^{tj} = \sum_{l=1}^{N_{wij}} \begin{Bmatrix} k_{1ij}^h[Y_s(x_{ijl}) + Y_h(x_{ijl})] \\ \quad +c_{1ij}^h[\dot{Y}_s(x_{ijl}) + \dot{Y}_h(x_{ijl})] \\ 2a_i^2[k_{1ij}^v\theta_s(x_{ijl}) + c_{1ij}^v\dot{\theta}_s(x_{ijl})] \\ \quad h_{4i}[k_{1ij}^h Y_s(x_{ijl}) + c_{1ij}^h\dot{Y}_s(x_{ijl})] \\ 2\eta_l d_i[k_{1ij}^h Y_s(x_{ijl}) + c_{1ij}^h\dot{Y}_s(x_{ijl})] \\ k_{1ij}^v Z_s(x_{ijl}) + c_{1ij}^v\dot{Z}_s(x_{ijl}) \\ 2\eta_l d_i[k_{1ij}^v Z_s(x_{ijl}) + c_{1ij}^v\dot{Z}_s(x_{ijl})] \end{Bmatrix},$$

$$(i = 1, 2, \cdots N_v;\ j = 1, 2),$$

$$F_{bn} = \sum_{i=1}^{N_v}\sum_{j=1}^{2}\sum_{l=1}^{N_{wij}}\{[(\phi_{hijl}^n + h_{3i}\phi_{hijl}^n)k_{1ij}^h Y_s(x_{ijl}) + 2\phi_{\theta ijl}^n k_{1ij}^v a_i^2\theta_s(x_{ijl}) + \phi_{vijl}^n k_{1ij}^v Z_s(x_{ijl})] + \phi_{vijl}^n g[m_{wijl} + (0.5M_{ci} + M_{tij})/N_{wij}]\}, \quad (22)$$

where:

$$\Phi_{hijl}^{nm} = (\phi_{hijl}^n + h_{4i}\phi_{\theta ijl}^n)(\phi_{hijl}^m + h_{4i}\phi_{\theta ijl}^m),$$

$$\phi_{\theta ijl}^{nm} = \phi_{\theta ijl}^n\phi_{\theta ijl}^m,$$

$$\Phi_{vijl}^{nm} = (\phi_{vijl}^n + e_i\phi_{\theta ijl}^n)(\phi_{vijl}^m + e_i\phi_{\theta ijl}^m).$$

Since the coefficients, ϕ and Φ, are the functions of the positions of the wheels, they are always changing when the train is running on the bridge. The elements in the mass, damping and stiffness matrices are, thus, time-dependent. The dynamic equations of the vehicle-bridge system are actually second-order linear non-homogeneous differential equations with time-varying coefficients. These equations are solved, using the Newmark implicit integral algorithm with $\beta = 1/4$, in this study.

CASE STUDY

A computer program is written, based on the formulation derived above and is used to perform a case study. The case study concerns a long suspension bridge carrying a railway inside the bridge deck (see Figures 2 and 3). The main span of the bridge is 1377 m and the height of the tower is 206 m, measured from the base level to the tower saddle. The two main cables of 36 m apart in the north and south are accommodated by the four saddles located at the top of the tower legs in the main span. A three-dimensional finite element model of the bridge was established and the natural frequencies and mode shapes were computed [9].

The train concerned in the case study consists of 8 passenger coaches. The main parameters of the coach used in the case study are listed in Table 1.

The track vertical, lateral and torsional irregularities are taken into consideration by using the measured data from one of the main railways in China. The length of the measured data is 2500 m and the samples, of a length of 600 m, are plotted in Figure 4 for lateral and vertical irregularities.

Displayed in Figure 5a is the time history of the lateral displacement responses of the bridge at the middle main-span. The train speed in calculation is 70 km/h. It is seen that, when the train runs on the left side span, the bridge responses at the middle main-span are quite small; when the train travels on the main span, the bridge response becomes large. As the

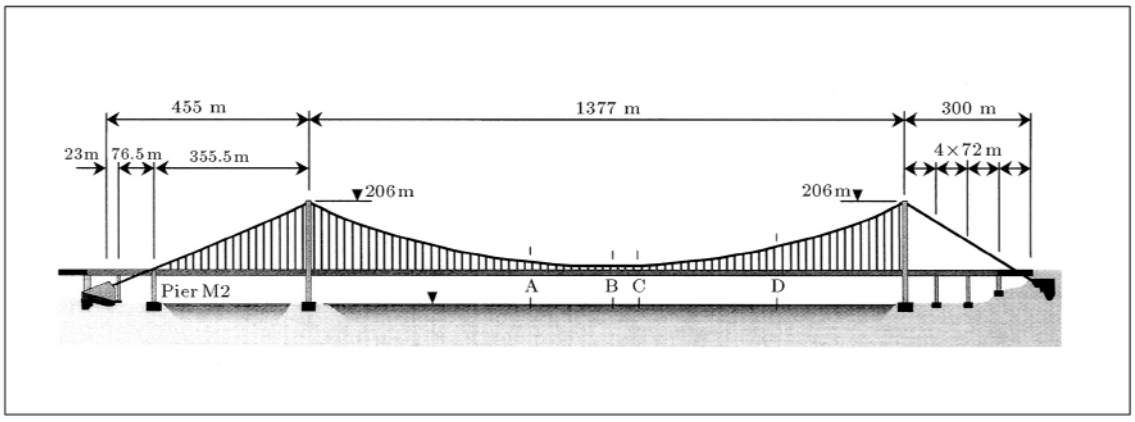

Figure 2. Configuration of the suspension bridge used in the case study.

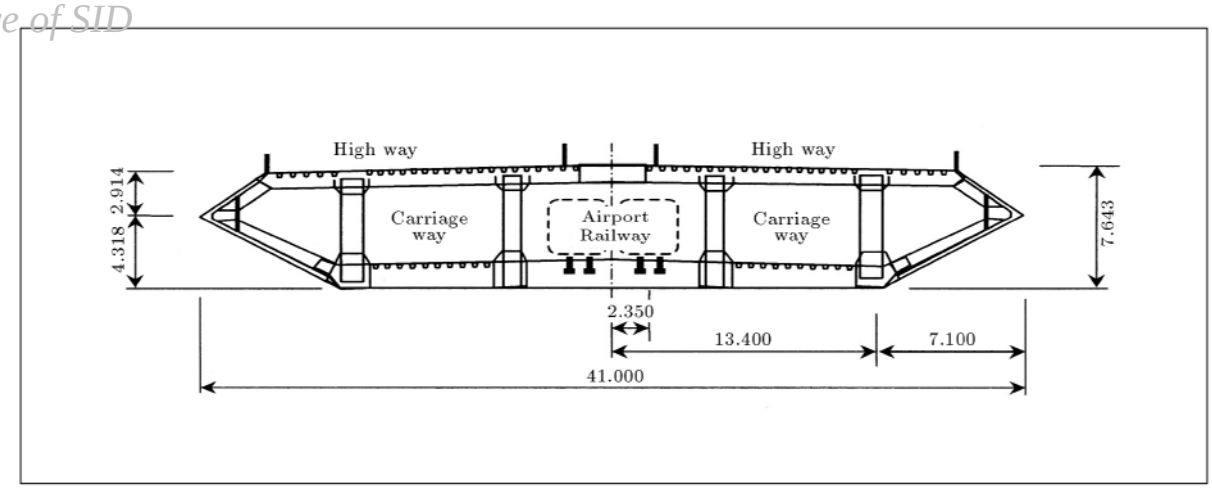

Figure 3. Cross section of bridge deck.

Table 1. Main parameters of the vehicle used in the case study.

Parameter	Unit	Value	Parameter	Unit	Value
Full length of a coach L	M	22.5	Secondary vertical spring stiffness k_2^v	kN/m	1060
Distance between bogies $2s$	M	15.6	Secondary lateral spring stiffness k_2^h	kN/m	460
Distance between wheel-sets $2d$	m	2.5	Primary vertical dashpot c_1^v	kNs/m	15
Mass of car body M_c	t	50.99	Primary lateral dashpot c_1^h	kNs/m	15
Car body roll mass moment $J_{c\theta}$	t-m^2	154.83	Secondary vertical dashpot c_2^v	kNs/m	30
Car body pitch mass moment of $J_{c\varphi}$	t-m^2	1958.7	Secondary lateral dashpot c_2^h	kNs/m	30
Car body yaw mass moment $J_{c\psi}$	t-m^2	1875.3	Distance h_1	M	0.98
Mass of bogie M_t	t	4.36	Distance h_2	M	0.36
Roll mass moment of bogie $J_{c\theta}$	t-m^2	1.47	Distance h_3	M	0.07
Pitch mass moment of bogie $J_{c\varphi}$	t-m^2	3.43	Distance h_4	m	1.25
Yaw mass moment of bogie $J_{c\psi}$	t-m^2	5.07	Distance a	m	0.98
Mass of wheel-set m_w	t	1.77	Distance b	m	1.12
Roll mass moment of wheel-set J_w	t-m^2	0.92	Distance B	m	1.435
Primary vertical spring stiffness k_1^v	kN/m	2976	Distance e	m	2.05
Primary lateral spring stiffness k_1^h	kN/m	20000			

train travels on the right side span, the bridge response decreases. The bridge, then, has a free vibration when the train leaves from the bridge. Figure 5b shows the corresponding response spectrum. There is a peak in the displacement response spectrum around 0.068 Hz, indicating that the first lateral vibration mode dominates the lateral displacement response. Nevertheless, the lateral displacement responses are quite small. In consideration of the fact that the track irregularities are the only excitation source to the bridge from the train, it can be, thus, concluded that the bridge lateral responses, due to track irregularities, are not significant.

Figure 6a shows the vertical displacement response of the bridge at four different positions. The distances of points A, B, C and D from the left abutment of the bridge are, respectively, 1012.5 m, 1138.0 m, 1174.0 m and 1498.5 m. The maximum vertical displacement response at each point occurs almost when the train runs around that point. The pattern of

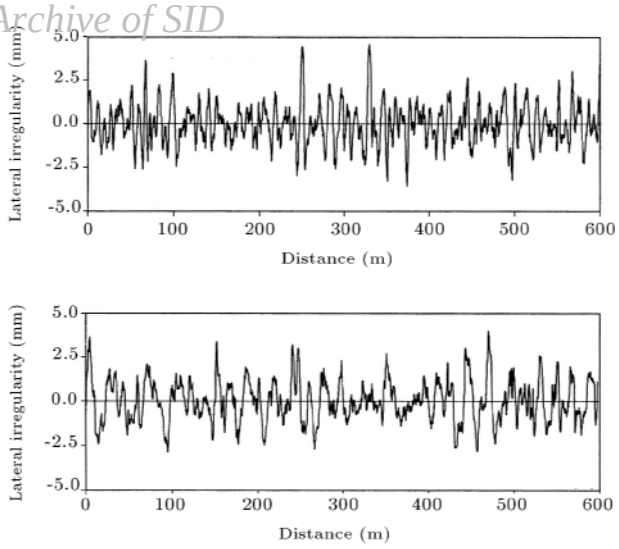

Figure 4. Measured track irregularity curves used in the case study.

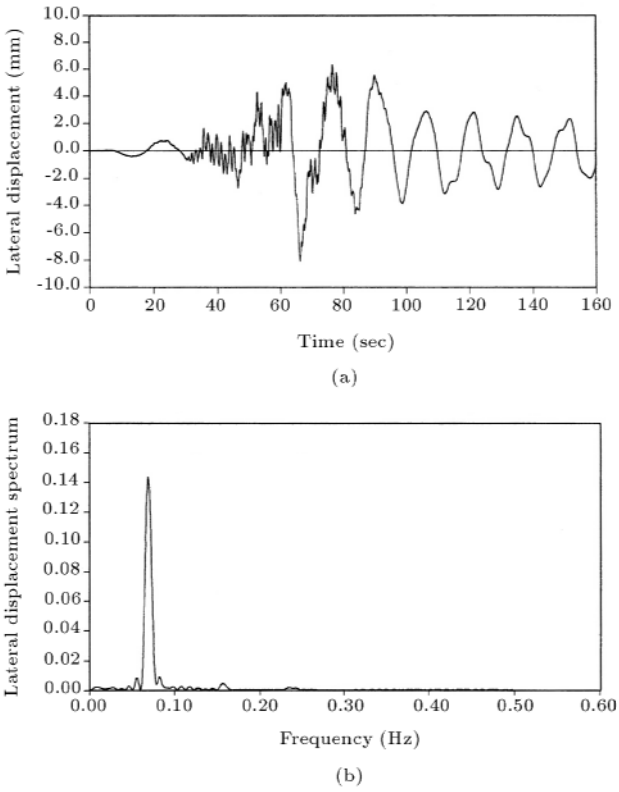

Figure 5. Lateral bridge responses.

the displacement response, however, depends on the position concerned. For instance, the displacement response curves of points A and D are clearly different from those at positions B and C. It is also seen that the maximum response at point D is larger than that at point C, which may be because the first vertical mode of vibration of the bridge is almost anti-symmetrical. Although the maximum vertical displacement response

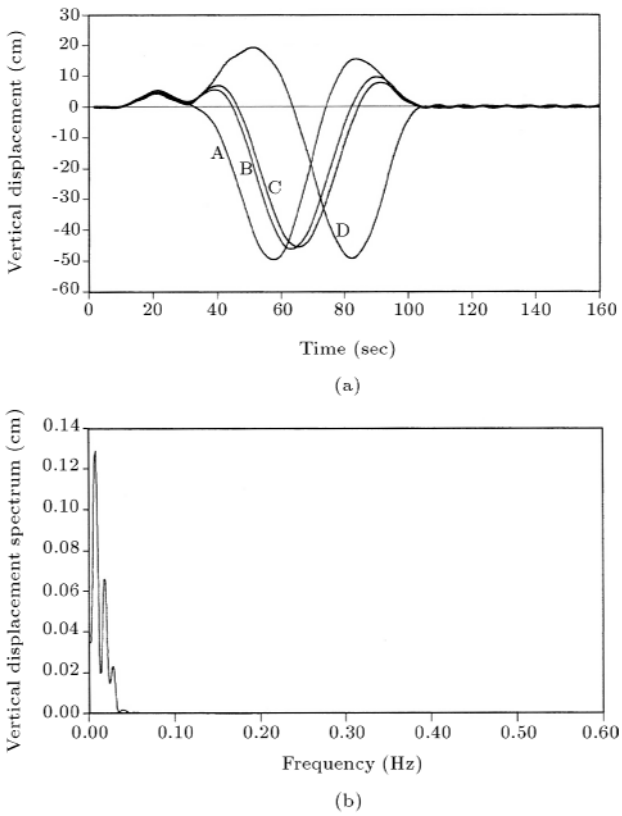

Figure 6. Vertical bridge responses.

at point C reaches 0.5 m, it is still very small compared with the main span of 1377 m long.

The bridge and train responses are computed for the train running at different speeds. The maximum lateral and vertical displacement and acceleration responses of the bridge are listed in Table 2. It is seen that the maximum vertical displacement response, the maximum lateral acceleration response and the maximum vertical acceleration response of the bridge increase with the increasing train speed, but, the maximum lateral displacement response decreases with the increasing train speed.

The maximum responses of the vehicle acceleration, wheel derail factor and offload factor are also listed in Table 2. It is seen that the train responses increase significantly with the increasing train speed.

To investigate the traffic-induced vibration of the bridge, two dynamic displacement transducers were installed on the bridge deck at the middle main span near the edge of the bridge deck. The measurement time was 45 minutes and the traffic on the bridge during the measurement included both highway and railway vehicles. Since the used dynamic displacement transducer could not measure the bridge response of very low frequency, due to the passage of the train, the direct comparison of the vertical dynamic displacement response between the measurement and the prediction could not be made. Figure 7 shows the measured

Table 2. Maximum responses of bridge and vehicles.

Types of Response	Unit	$U = 20$ km/h	$U = 40$ km/h	$U = 70$ km/h	$U = 120$ km/h
Deck vertical displacement	cm	49.39	49.52	51.29	54.04
Deck vertical acceleration	cm/s^2	0.0845	0.332	0.878	3.156
Deck lateral displacement	mm	15.07	10.83	8.058	4.686
Deck lateral acceleration	cm/s^2	0.931	1.097	1.298	2.234
Vehicle vertical acceleration	cm/s^2	12.96	31.85	48.29	74.31
Vehicle lateral acceleration	cm/s^2	19.01	38.19	40.05	51.92
Derail factor	Q/P	0.247	0.287	0.306	0.413
Offload factor	$\Delta P/P$	0.380	0.381	0.393	0.410

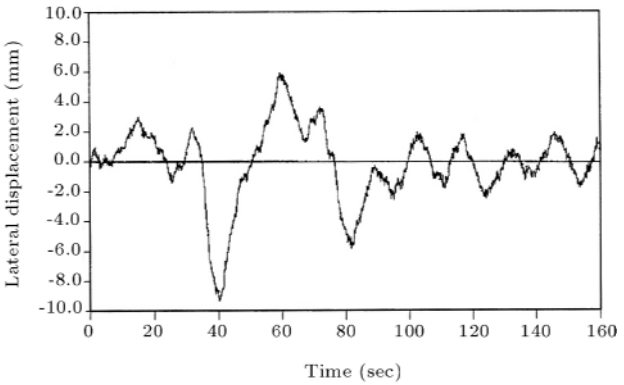

Figure 7. Measured bridge lateral displacement.

lateral dynamic displacement response of the bridge at the middle main span during the passage of the train. It is seen that the predicted vibration pattern and the amplitude of the lateral displacement response (Figure 7) are similar to those from the measurement, although they are not exactly the same. Both lateral response curves also exhibit a kind of random vibration nature.

CONCLUSIONS

In this paper, a formulation has been developed for investigating the dynamic interaction of a long suspension bridge under running trains. Each railway vehicle was modeled as a 27 degrees-of-freedom dynamic system and a three-dimensional dynamic finite element model was developed to represent the suspension bridge. To reduce the degrees of freedom of the coupled bridge-train system, due to track irregularities and contact forces between the wheels and track, this study took the measured track irregularities as known quantities and applied the mode superposition technique for the analysis of the bridge. A real long suspension bridge carrying a train inside the bridge deck was taken as a case study. The dynamic response of the bridge-train system and the derail factor and the offload factor related to the running safety of the train were computed. The calculated lateral displacement response of the bridge was also compared with the measured data. The results showed that the formulation presented in this paper could well predict the dynamic behaviors of both the bridge and train with reasonable computation effort. It was also found that the dynamic responses of the long suspension bridge under the running train are relatively small and the effects of bridge motion on the runability of the railway vehicles are insignificant.

ACKNOWLEDGMENTS

The authors are grateful for the financial support of the Natural Science Foundation of China and the Hong Kong Polytechnic University through an internal research grant. The support from the MTR Corporation, Hong Kong Limited, in providing the writers with the relevant vehicle information, is particularly appreciated.

REFERENCES

1. Gimsing, N.J., *Cable Supported Bridges*, John Wiley & Sons, Chichester, England (1997).
2. Beard, A.S. and Young, J.S. "Aspect of the design of the Tsing Ma Bridge", *Proc. Int. Conf. on Bridge into 21st Century*, Impressions Design & Print Ltd., Hong Kong, pp 93-100 (1995).
3. Diana, G. and Cheli, F. "Dynamic interaction of railway systems with large bridges", *Vehicle System Dynamics*, **18**, pp 71-106 (1989).
4. Fryba, L., *Dynamics of Railway Bridges*, Thomas Telord, London, England (1996).
5. Xia, H. "Characteristics of traffic induced vibrations and their effects on environments", H. Xia, G. De

Roeck, Eds., in *Traffic Induced Vibrations & Controls*, NJTU Press, Beijing, pp 83-90 (2001).

6. Yasoshima, Y., Matsumoto, Y. and Nishioka, T. "Studies on the running stability of a railway vehicle on suspension bridges", *J. Fac. of Eng.*, Tokyo Univ., Japan, **XXXVI** (1981).

7. Xia, H. and Chen, Y.J. "Dynamic analysis of steel truss bridges under moving train loads", *Advances in Structural Engineering*, Xia and Chen, Eds., China Railway Publishing House, Beijing, China, pp 48-54 (1995).

8. Xia, H., Zhang, H. and De Roeck, G. "Dynamic analysis of train-bridge system under random excitations", *Proc. 4th Int. Conf. on Stochastic Struc. Dyn.*, Notre Dame, USA, Rotterdam, Balkema, pp 535-542 (1998).

9. Xu, Y.L., Ko, J.M. and Zhang, W.S. "Vibration studies of Tsing Ma suspension Bridge", *J. Bridge Engineering, ASCE*, **3**(4), pp 149-156 (1997).